

# Structure and Strength of Dislocation Junctions: An Atomic Level Analysis

D. Rodney and R. Phillips

*Division of Engineering, Brown University, Providence, RI 02912*

(October 11, 2018)

The quasicontinuum method is used to simulate three-dimensional Lomer-Cottrell junctions both in the absence and in the presence of an applied stress. The simulations show that this type of junction is destroyed by an unzipping mechanism in which the dislocations that form the junction are gradually pulled apart along the junction segment. The calculated critical stress needed for breaking the junction is comparable to that predicted by line tension models. The simulations also demonstrate a strong influence of the initial dislocation line directions on the breaking mechanism, an effect that is neglected in the macroscopic treatment of the hardening effect of junctions.

The mechanical properties of a wide range of materials can be traced in part to the motion and interaction of dislocations. Dislocation junctions serve as one class of obstacles to dislocation motion. From the standpoint of work hardening, junctions have been implicated as a primary contributor to the observed increase in the flow stress with increasing dislocation density [1]. They are one example of "dislocation chemistry" in which dislocations can join and dissociate to form new segments. Such reactions involve both atomic and elastic effects since in the core regions there are substantial atomic rearrangements, while at larger distances the dislocations still interact elastically.

Until now, the vast majority of information concerning dislocation junctions has been obtained either from macroscopic hardening experiments [2] or models deriving from elasticity theory [3,4]. On the other hand, evidence has been mounting for decades that in certain circumstances dislocation core effects play a critical role in determining the actual behavior of materials [5], and recent calculations have shown that atomic level insights can be gained with respect to junctions as well [6]. The calculations undertaken here attempt to account for both the long range elastic interactions and the detailed atomic level geometries that give junctions their overall behavior. Though we have made a systematic study of a number of dislocation junctions found in fcc materials, we concentrate here only on the case of the Lomer-Cottrell junction. Our reason for limiting the discussion is the presumed importance of the Lomer-Cottrell junction in governing the hardening of fcc materials as deduced from experimental analyses [2].

Our ambition in the pages that follow is to examine the atomic-level structure of the Lomer-Cottrell junction both in the absence and presence of an externally applied stress. The response of a junction to an applied stress is of prime importance since, in macroscopic descriptions of hardening [7], obstacles to dislocation motion such as junctions are represented by parameters derived from the stress needed to force the dislocations across the obstacles of interest.

Although such an investigation demands an atomic level calculation, it is also evident that three-dimensional calculations of this sort require an enormous compu-

tational investment. As an alternative to full-scale atomistic simulations, we have used the quasicontinuum method [8] as the primary vehicle for our analysis. By linking finite element discretization with atomic level calculations it is possible to carry out simulations in which only small neighborhoods of the dislocation slip planes are treated with full atomic resolution, while in the far fields a coarser finite element mesh is exploited. In order to make sure that there were no mesh effects, we performed simulations on the same geometries with varying atomistic regions.

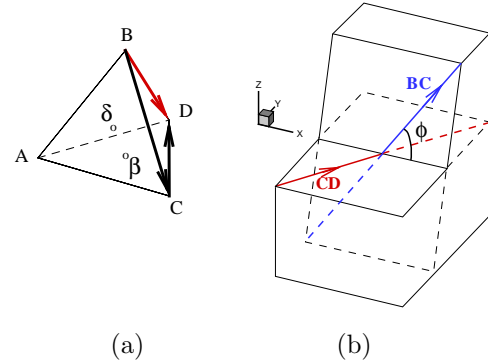


FIG. 1. (a) Thompson tetrahedron illustrating the Burgers vectors of the dislocations of interest. (b) Schematic section of the initial simulation cell along the glide planes of the dislocations. The two dislocations have the same length,  $2l$ , and make the same angle  $\phi$  with the line of intersection between the glide planes.

The basic elements of our simulations are carried out as follows. The geometry is best understood by appealing to fig. 1. The Thompson tetrahedron shown in fig. 1(a) is used to characterize the possible dislocations that can form in an fcc material. We consider the case of two interacting  $a/2\langle 110 \rangle\{111\}$  dislocations shown schematically in fig. 1(b). The first dislocation lives in the horizontal ACD plane also labeled  $\beta$  in fig. 1(a) and has a Burgers vector equal to the vector  $CD$ . We imagine that this dislocation interacts with a partner dislocation in the inclined slip plane ABC (labelled  $\delta$ ) with a Burgers vector  $BC$ . The Burgers vector of the junction segment

is the sum of the initial vectors. From the Thompson tetrahedron, it is obvious that this vector is  $\mathbf{BD}$  which is in neither of the initial glide planes. The significance of this observation is that the resulting junction is expected to be sessile since it can glide in neither of the relevant slip planes. As a result, this type of junction is expected to impede the motion of the dislocations and therefore is a source of hardening.

To carry out the simulations, the dislocations are installed in a simulation cell by virtue of their linear elastic fields. All the nodes of the mesh are displaced in accordance with the superposition of the Volterra fields due to the two participating dislocations. Typical cell dimensions are of the order of  $(300\text{\AA})^3$ . A typical simulation demands around  $1.5 \times 10^5$  representative atoms, in contrast with the  $1.5 \times 10^6$  atoms that would be required to carry out a conventional lattice statics simulation with the same geometry. The dislocations are initially straight and undissociated. We have chosen a highly symmetric geometry in which the angle between the dislocations and the line of intersection of the two glide planes is  $\phi = 60^\circ$  and the two dislocations have the same length  $2l$ . This idealized geometry is similar to that envisaged in elastic models for junction formation [3,4] and therefore lends itself to direct comparison with such models. Simulations were performed with dislocation lengths equal to 300 and 400  $\text{\AA}$ .

The initial separation between the dislocations is 6  $\text{\AA}$  leading to a strong mutual interaction. The atoms on the boundary of the computational cell are held fixed in accordance with their initial elastic displacements. Because of these rigid boundary conditions, the dislocations are pinned at their ends. The equilibrium structure is then determined as the energy minimizing configuration (obtained by conjugate gradients) associated with the boundary conditions of interest. For the purposes of the present analysis, we have exploited the embedded atom (EAM) potentials of Ercolessi and Adams [9] developed to simulate aluminum crystals.

In order to garner some idea of the role of finite size effects, it is useful to estimate the magnitude of the dislocation densities corresponding to the geometry present in our simulations. We can imagine that the dislocations are pinned on the surfaces of the simulation cell because they take part in other junctions at these points. The distance between the junctions in this imaginary network is therefore close to 150  $\text{\AA}$ . The classical relation coupling the mean separation between pinning points and the density of dislocations yields  $\rho \sim 1/l^2 \sim 10^{15} m^{-2}$  which corresponds to the upper limit for densities in heavily worked materials.

For the purposes of examining the action of an applied stress and to force the horizontal dislocation in plane  $\beta$  to glide through the inclined one, we have carried out a sequence of quasistatic calculations in which the simulation cell itself is subjected to incremental shears. A homogeneous shear  $\gamma_{yz} = \partial u_y / \partial z = \text{constant}$  is applied in increments of 0.27%. In the linear elastic approximation, this deformation corresponds to resolved shear stresses equal

to  $\frac{\sqrt{3}}{2}\mu\gamma_{yz}$  on the horizontal dislocation and  $\frac{7}{6\sqrt{3}}\mu\gamma_{yz}$  on the inclined one. As will be shown below, the strains at which the junctions break are of order of 2%, which may well exceed the limits of validity of the linear elastic approximation suggested above. For each load step, the energy is minimized, with the result that a series of equilibrium states under increasing applied stress are obtained. The results of the simulations are visualized by plotting only those atoms whose energy exceeds that of atoms in the middle of a stacking fault.

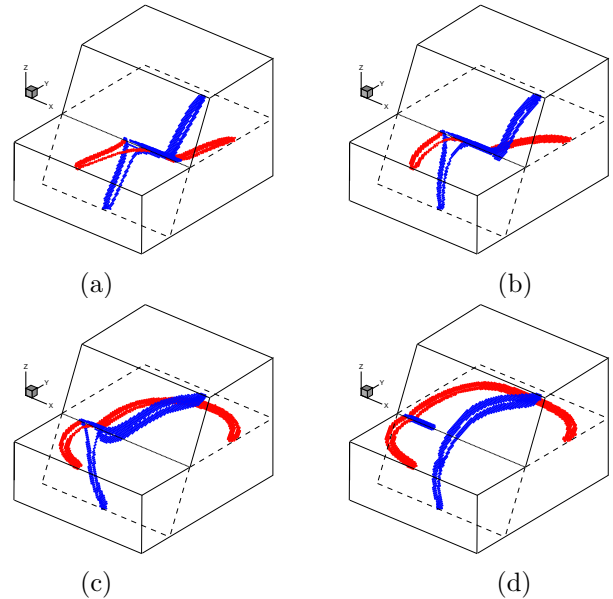


FIG. 2. Sequence of snapshots of the junction geometry under increasing stress. (a) Zero applied stress, (b) stress is  $0.011\mu$ , (c) stress is  $0.018\mu$  just before the junction breaks, (d) stress is  $0.018\mu$  at the end of the simulation.

Fig. 2 shows the disposition of the junction at four stages of deformation. Fig. 2(a) illustrates the structure in the absence of any applied stress, with the result that a junction is formed along the line of intersection between the glide planes of the initial dislocations. The four arms of the junction are dissociated in their glide planes as is evidenced by the presence of two segments on each arm which are Shockley partials. The Burgers vectors of all of the dislocation segments can be computed from the Burgers vectors of the initial segments and the vectors of the stacking faults. The junction segment itself is built up of two parts. A stair-rod Lomer-Cottrell segment with a Burgers vector  $\delta\mathbf{b}$  of the type  $a/6\langle 110 \rangle$  (see fig. 1(a)) forms one edge of the extended node on the left side of the junction. The remaining part of the junction segment is a Lomer dislocation with Burgers vector  $\mathbf{BD}$  as expected from the crystallographic analysis given above. The nature of this dislocation is also evidenced by its five-fold symmetrical core which is seen on closer inspection of the atomic region. Unlike the left hand node, the right hand node is pointlike and is the meeting point of the constricted segments. The size of the extended node is independent of the initial dislocation length and of the initial angle  $\phi$  and is therefore dictated

by the equilibrium of the incoming partials only. On the other hand, the simulations show that the length of the Lomer segment increases with decreasing initial angle  $\phi$  and increasing dislocation length. This latter result was expected on the basis of elastic models [3].

The detailed structure of the junction itself involves other interesting features as well. Kinematic arguments [10] predict that dislocations acquire a step after passing through each other, whose height is equal to the Burgers vector of the dislocation being crossed. In the present setting, even in the initial stress free configuration, this discontinuity is present in the sense that arms of the junction which once formed a single dislocation, for example the two horizontal arms, already live on *different* parallel  $\{111\}$  planes. The origin of this structure is the discontinuity of the deformation across both glide planes behind the dislocations.

The results of our simulations can be considered in light of both earlier experimental and theoretical work. The global structure as well as the fact that the junction is along the line of intersection between glide planes agrees with the assumed structures of the elastic models. Moreover the calculated junction is compatible with TEM observations [11,12] made on AlCu alloys with low stacking fault energies. The major difference between our results and those found in the experiments is the existence in the simulations of the undissociated Lomer segment. In the experiments, the entire length of the junction segment is dissociated. On the other hand, this effect can be rationalized by appealing to the relatively high stacking fault energy associated with the EAM potentials used here.

The simplest elastic model (based on a uniform line tension approximation [3]) allows for a three-dimensional generalization of Frank's rule (which states that in two dimensions two dislocations will combine if  $\mathbf{b}_1 \cdot \mathbf{b}_2 < 0$ ) such that a junction will form not only if the Burgers vectors satisfy a similar condition, but also if the initial angle  $\phi$  is less than some critical value. In fact, the geometry considered above corresponds to an initial angle which is precisely the critical angle separating those for which a junction forms from those in which there is no junction formation. An important future direction for this type of analysis is to make a systematic study of the tendency towards junction formation as a function of this initial angle.

In addition to shedding light on the propensity for stable junction formation, elastic models can also be used in order to examine the stability of such junctions under the action of an applied stress. The models predict that (1) the arms bow out under the applied stress, (2) the junction translates along the line of intersection and (3) its length decreases monotonically with increasing stress via an 'unzipping' mechanism. Unzipping takes place as the two dislocations forming the junction segment are pulled apart under the action of the applied stress. The models also predict that, depending on the dislocation line directions, there exists either a stress where the length of the junction becomes zero or a stress above which the

junction is unstable. The junction is destroyed if either of these critical stresses is reached. Line tension models show that the critical stress to break the junction decreases as the length of the junction arms increases. In particular, with a uniform line tension, in the configuration envisaged in the simulations, the critical resolved shear stress averaged over all possible line directions is estimated to be  $\sim 0.5\mu b/l$  where  $l$  is the length of the dislocation arms.

The mechanism for destruction of the junction observed in the simulations is similar to that envisaged in the elastic models. As can be seen in fig. 2(b), (c) and (d), each arm bows out as a result of the non zero resolved shear stresses on both of the dislocations. With increasing stress, the junction segment translates along the line of intersection between glide planes but does not bow out itself, confirming the fact that the junction is a sessile lock. Between  $\sigma = 0$  and  $\sigma = 0.011\mu$ , the length of the Lomer segment increases in contrast with the predictions of the elastic models which predict that the length of the junction segment decreases monotonically with increasing stress. After this point, with increasing stress, the length of the Lomer segment decreases until the stress reaches a value of  $\sigma = 0.018\mu$ , at which point the Lomer segment disappears in keeping with the unzipping mechanism in which the junction length decreases until it vanishes altogether. The net result of the breaking of the junction is that the dislocation in the horizontal glide plane is now a fully bowed out single dislocation, while the dislocation on the inclined plane snaps back to a more nearly straight configuration because of the lower resolved shear stress associated with that dislocation.

Other consequences of the passage of the horizontal dislocation through the other can be observed in the simulations. In particular, a tube of energetic atoms forms behind the horizontal dislocation. The simulations show that this is a tube of vacancies which originate from the step that forms on the horizontal dislocation when the junction breaks. As mentioned earlier, the arms of the dislocation live on different  $\{111\}$  planes with the consequence that when they join to reconstruct the initial dislocation, the latter acquires a jog whose height is equal to the interplanar spacing. It can be seen from the simulations that the jog on the horizontal dislocation is sessile. As the dislocation expands, it leaves behind a dislocation dipole which is equivalent to a tube of vacancies since its height is only an interplanar spacing. As no temperature effects are accounted for in the simulations, the vacancies cannot diffuse away and remain along the tube. Similarly a jog forms on the inclined dislocation. In this case, the jog is constricted and glissile. Its motion along its glide plane (the BCD plane of fig. 1(a)) can be followed in the simulations.

From a quantitative viewpoint, our simulations reveal that the critical resolved shear stress for breaking the junction is  $\sigma_c = 0.017\mu = 0.8\mu b/l$  where  $l$  is the dislocation arm length. This value is of the same order as those determined on the basis of the elastic models. Note however that there exists important differences between the

calculated configurations and what was expected from the models. For example, the deformations observed are much larger than the limit of validity of the line tension approximation. Moreover the wavy structure of the inclined arm in fig. 2(c) cannot be explained in a line tension approximation and is due to a core effect of the junction.

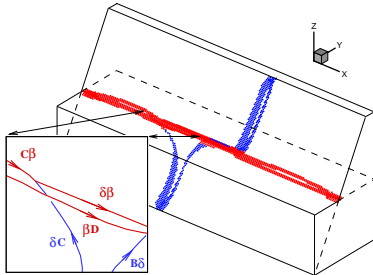


FIG. 3. Structure of a second Lomer-Cottrell junction in the absence of applied stress. The inset is a close-up showing schematically the configuration of the extended node. The vectors refer to the Burger vectors of the dislocation segments

The nature of a junction geometry and the mechanisms whereby the junction is destroyed are significantly affected by the line direction of the parent dislocations as well. This point is made more clear by appeal to fig. 3 in which we show the results for exactly the same junction type as considered earlier, but now with a horizontal dislocation initially along the line of intersection between glide planes.

A particularly interesting feature of the second geometry is the distinct mechanism that is associated with the destruction of the junction. As before, a junction forms along the line of intersection between glide planes. The right end is constricted while the one on the left is extended with the difference that in this case one of the Shockley partials is alongside the junction segment itself. Their separation is small and no perfect stacking fault forms in this region. The inset in fig. 3 is a schematic view of the configuration near the extended node which shows both the junction segment  $\delta\beta$  and the  $\beta D$  Shockley partial. In the presence of the applied stress, the arms bow out as previously described. After the length of the Lomer segment increases, it begins to unzip, but becomes unstable before it has completely disappeared. The applied stress pushes the Shockley partial mentioned above against the Lomer-Cottrell segment. The junction becomes unstable when the stress becomes high enough to force the "re-association" of the  $\delta\beta$  and  $\beta D$  segments. Note however that this instability is not of the same nature as the one predicted by the elastic models. Here, its origin is the equilibrium of the extended node and is related to the dissociation of the dislocations which is not taken into account in the models. Once the junction is destroyed, jogs appear on both dislocations.

The results of our analysis demonstrate that much of the intuition built up concerning junctions on the basis

of line tension models are borne out qualitatively in the context of detailed atomic level analyses. On the other hand, from a quantitative standpoint, we have found that the stability of junctions both in the absence and in the presence of an applied stress can be quite different from the simplest elastic estimates. The logical extension of the work begun here will be to effect a series of systematic studies on the role of the initial angle between the participating dislocations in governing the propensity for junction formation and the role of the junction arm lengths in determining the critical stress for breaking the junction. In addition, it remains an outstanding challenge to continue efforts [13] to link the type of analysis made here to higher level models of dislocation motion in which dislocations are presumed to interact with obstacles to slip that are characterized by nothing more than a breaking force such as the one evaluated in the present work.

We acknowledge many helpful and illuminating discussions with J. Bassani, V. Bulatov, G. Canova, M. Fivel, M. Ortiz, G. Saada and V.B. Shenoy. In addition, we gratefully acknowledge the support of Electricité de France, the NSF supported MRSEC at Brown University, and the Caltech ASCI program.

- 
- [1] S.J. Basinski and Z.S. Basinski, in F.R.N. Nabarro (ed.), *Dislocations in Solids*, vol. 4, North-Holland Amsterdam, 261 (1979).
  - [2] P. Franciosi, M. Berveiller and A. Zaoui, *Acta Met.*, **28**, 273 (1980).
  - [3] G. Saada, *Acta Met.*, **8**, 841 (1960).
  - [4] G. Schoeck and R. Frydman, *Phys. Stat. Sol.*, **53**, 661 (1972).
  - [5] V. Vitek, D. Pope and J. Bassani, *Dislocations in Solids*, edited by F. R. N. Nabarro and M. S. Duesbery, vol. 10, North-Holland Amsterdam, (1996).
  - [6] S.J. Zhou, D.L. Preston, P.S. Lomdahl and D.M. Beazley, *Science*, **279**, 1525 (1998).
  - [7] U.F. Kocks, *Phil. Mag.*, **13**, 541 (1966).
  - [8] E.B. Tadmor, M. Ortiz, and R. Phillips, *Phil. Mag.*, **A73**, 1529 (1996); V.B. Shenoy, R. Miller, E.B. Tadmor, R. Phillips and M. Ortiz, *Phys. Rev. Lett.*, **80**, 4, 742 (1997).
  - [9] F. Ercolessi and J.B. Adams, *Europhys. Lett.*, **26**, 583 (1994).
  - [10] R.D. Heidenreich and W. Shockley, Bristol conference, Phys. Soc., London (1948).
  - [11] S. Amelynckx, in F.R.N. Nabarro (ed.), *Dislocations in Solids*, vol. 2, North-Holland Amsterdam, 67 (1979).
  - [12] H.P. Karnthaler and E. Wintner, *Acta Met.*, **23**, 1501 (1975).
  - [13] V. Bulatov, F. Abraham, L. Kubin, B. Devincre and S. Yip, *Nature*, **391**, 669 (1998).